Recent Developments in Direct Methods of Solving Crystal Structures

By Fan Hai-fu

Institute of Physics, Chinese Academy of Sciences, Beijing 100080, P.R. China
Department of Physics, Zhongshan University, Guangzhou 510275
Laboratory of Structure Analysis, University of Science and Technology of China, Hefei 230026

1. The phase problem in diffraction analysis for solving crystal structures

In diffraction analysis, a crystal structure is represented by a general distribution of scattering density $\rho(\mathbf{r})$. In the case of X-ray diffraction $\rho(\mathbf{r})$ is the electron density function, while in the case of electron diffraction it is the potential distribution. The relative scattering amplitude of a unit cell is expressed by the structure factor $F(\mathbf{H})$. Neglecting the dynamical diffraction effect $F(\mathbf{H})$ is given by the Fourier transform of $\rho(\mathbf{r})$:

$$F(\mathbf{H}) = \int_V \rho(\mathbf{r})\exp(i2\pi\mathbf{H}.\mathbf{r})dv$$

or

$$F(\mathbf{H}) = \sum_j f_j \exp(i2\pi\mathbf{H}.\mathbf{r}_j) \quad . \qquad (1)$$

Where $\mathbf{H}$ is a position vector in reciprocal space, i.e. the diffraction vector of $F(\mathbf{H})$; $\mathbf{r}$ is a position vector in direct space; V is the volume of the unit cell; f_j and $\mathbf{r}_j$ are respectively the atomic scattering factor and the position vector of the jth atom within a unit cell. From (1) according to the Fourier transform theorem we have

$$\rho(\mathbf{r}) = \int_\tau F(\mathbf{H})\exp(-i2\pi\mathbf{H}.\mathbf{r})d\tau$$

or

$$\rho(\mathbf{r}) = \sum_H F(\mathbf{H})\exp(-i2\pi\mathbf{H}.\mathbf{r}) \quad . \qquad (2)$$

Here τ denotes the entire reciprocal space. Usually $F(\mathbf{H})$ is a complex quantity and can be written as

$$F(\mathbf{H}) = |F(\mathbf{H})|\exp(i\varphi_H) \quad . \qquad (3)$$

If one can measure from a diffraction experiment the whole set of structure factors F(**H**), including the magnitudes and phases, then the crystal structure analysis will be a straightforward task by calculating $\rho(\mathbf{r})$ from (2). However from the experiment only the magnitudes |F(**H**)| but not the phases φ_H of structure factors can be obtained. Hence one has to recover the lost phases before equation (2) can be used. This is the well-known "phase problem" in diffraction analysis.

2. Direct methods in crystallography

Direct methods is that kind of method which can retrieve the "lost" phases φ_H directly from a set of structure factor magnitudes |F(**H**)|. The mathematical basis of this is seen from equation (1) which can be split into the real and imaginary parts by making use of (3), i.e.

$$|F(\mathbf{H})|\cos\varphi_H = \sum_j f_j \cos(2\pi\mathbf{H}.\mathbf{r}_j)$$

and

$$|F(\mathbf{H})|\sin\varphi_H = \sum_j f_j \sin(2\pi\mathbf{H}.\mathbf{r}_j) \quad . \qquad (4)$$

The unknown quantities in (4) are the phase angle φ_H and the atomic coordinates x_j, y_j and z_j ($\mathbf{r}_j = x_j\mathbf{a} + y_j\mathbf{b} + z_j\mathbf{c}$; **a**, **b** and **c** are vectors defining the unit cell). Each measured magnitude |F(**H**)| gives two simultaneous equations and at the same time introduces one unknown quantity φ_H. Suppose that there are 300 independent atoms in the unit cell. Then there will be 900 unknown atomic coordinates. By measuring the magnitudes of 900 independent structure factors we can set up 1800 simultaneous equations, which are in principle sufficient to solve all the unknown quantities --- 900 phases and 900 atomic coordinates. In the case of X-ray diffraction, for a crystal of moderate complexity it is trivial to collect intensities of thousands of independent reflections. Therefore the phase problem and the crystal structure are over-determined by the whole set of structure factor magnitudes |F(**H**)|. Nevertheless crystal structures are not really determined by solving the simultaneous equations (4). Special mathematical approaches are used in direct methods to derive phases of structure factors from a set of structure factor magnitudes |F(**H**)|. The crystal structure is then revealed on the map calculated from (2).

One of the fundamental formulae of direct methods is the Sayre equation (Sayre, 1952), which describes the relationship among structure factors, including phases and magnitudes:

$$F(\mathbf{H}) = (\Theta/V) \sum_{H'} F(\mathbf{H'})F(\mathbf{H}-\mathbf{H'}) \quad , \qquad (5)$$

where Θ is an atomic form factor and V the volume of a unit cell. The summation is over the entire reciprocal space. In theory the Sayre equation is valid only under the following conditions:

i) $\rho(\mathbf{r})$ is everywhere positive;

ii) the crystal consists of discrete atoms which do not overlap each other;

iii) there are only one kind of atoms in the crystal.

In practice conditions i and ii are nearly true for both X-ray and electron diffraction, while the condition iii could seldom be satisfied. The deviation from condition iii just gives rise to the "squaring effect" which renders, in the resultant map $\rho(\mathbf{r})$, the heavy atoms much heavier while the light atoms much lighter than they should be.

The most widely-used formula in direct methods is probably the tangent formula (Karle & Hauptman, 1956):

$$\tan \varphi(\mathbf{H}) \approx$$

$$\sum_{H'} |E(\mathbf{H'})E(\mathbf{H}-\mathbf{H'})| \sin\{\varphi(\mathbf{H'})+\varphi(\mathbf{H}-\mathbf{H'})\} \Big/ \sum_{H'} |E(\mathbf{H'})E(\mathbf{H}-\mathbf{H'})| \sin\{\varphi(\mathbf{H'})+\varphi(\mathbf{H}-\mathbf{H'})\}, \qquad (6)$$

where $E(\mathbf{H})$ is the normalized structure factor, the magnitude of which can be obtained through $|F(\mathbf{H})|$. The tangent formula can be regarded as the angular portion of Sayre's equation, however unlike the Sayre equation, the summation $\Sigma_{H'}$ in the tangent formula can be composed of a small number of terms and the validity of the formula is evaluated by a probability distribution given by Cochran (1955):

$$P(\Phi_3) = \{1/2\pi I_o(\kappa)\} \exp\{\Sigma_{H'} (\kappa \cos\Phi_3)\} \quad , \qquad (7)$$

where

$$\Phi_3 = \varphi(\mathbf{H}) - \varphi(\mathbf{H'}) - \varphi(\mathbf{H}-\mathbf{H'}) \quad ,$$

$$\kappa = 2\sigma_3/\sigma_2^{3/2} |E(\mathbf{H})E(\mathbf{H'})E(\mathbf{H}-\mathbf{H'})| \quad ,$$

$$\sigma_n = \sum_j (Z_j)^n \quad ,$$

Z_j is the atomic number of the jth atom in a unit cell and I_o is the zero order of a family of modified Bessel functions, I_n.

At present systematic techniques of applying the tangent formula and the Sayre equation to solve crystal structures from X-ray diffraction data have been well established. Important contributions were made by Woolfson and his colleagues (Germain & Woolfson, 1968; Yao, 1981; Debaerdemaeker, Tate & Woolfson, 1985, 1988). With the latest techniques of direct methods most crystal structures of moderate complexity can be solved in a routine way.

3. Direct methods outside traditional field

Direct methods are so successful that their important contribution to science has been recognized by the award of the Nobel Prize for Chemistry to two pioneers of direct methods, H. Hauptman and J. Karle. On the other hand direct methods are still limited to the structure analysis of single crystals with moderate complexity using X-ray diffraction data. New application fields for direct methods remain to be explored. Recently direct methods are expanding along the following lines:

i) from the structure analysis of single crystals to that of polycrystalline samples;

ii) from ideal three-dimensional periodic structures to aperiodic structures, including incommensurate modulated structures and quasicrystals;

iii) from X-ray crystallography to electron microscopy;

iv) from small molecules to proteins.

In the following, examples will be given on the last three topics.

3.1 Direct methods for incommensurate modulated structures

A modulated structure can be regarded as the result of applying a periodic modulation to a regular structure. Fig. 1 shows two simplified examples. The modulation wave (fig. 1a) in the figure represents the fluctuation of atomic occupancy. When it is applied to the background regular structure, the "heights" of the atoms are modified. A commensurate modulated structure (superstructure) will result (fig. 1b) if the period T of the modulation function is commensurate with the period t of the structure, i.e. T/t=n, where n is an integer. The resulting superstructure now has a true period T and a pseudo period t, respectively corresponding to a true unit cell and a pseudo unit cell. On the other hand, if T is incommensurate with t (fig. 1c), i.e. T/t=r, where r is not an integer, we obtain an incommensurate modulated structure, in which no exact periodicity occurs, although t remains a pseudo period. A modulation function can also represent a fluctuation in atomic positions and the positional modulation can also be either commensurate or incommensurate. In practice a modulated structure can simultaneously include different kinds of occupational and/or positional modulations.

An incommensurate modulated structure produces a three-dimensional diffraction pattern, which contains satellites round the main reflections. An example of a section of such a three-dimensional diffraction pattern is shown schematically in fig. 2. The main reflections are consistent with a regular three-dimensional reciprocal lattice although the satellites do not fit the same lattice. On the other hand, although the satellites are not commensurate with the main reflections, they have their own periodicity. Hence, it can be imagined that the three-dimensional

diffraction pattern is a projection of a four-dimensional reciprocal lattice, in which the main and the satellite reflections are all regularly situated at the lattice nodes. From the properties of the Fourier transform the incommensurate modulated structure here considered can be regarded as a three-dimensional "section" of a four-dimensional periodic structure. The multi-dimensional representation of incommensurate modulated structures, which forms the basis of structure analysis in multi-dimensional space, was first proposed by de Wolff and further developed by Janner & Janssen (de Wolff, 1974; Janner & Janssen, 1977; de Wolff, Janssen & Janner, 1981).

Up to the present, studies of incommensurate modulated structures were mostly based on preliminary assumption of the modulation function. Direct methods have been extended for solving incommensurate modulated structures in multi-dimensional space. According to Hao, Lui & Fan (1987) the Sayre equation (5) is also valid for a multi-dimensional periodic structure with the reciprocal vector **H** defined in a multi-dimensional space. The right-hand side of equation (5) can be split into three parts:

$$F(\mathbf{H}) = (\Theta/V) \sum_{H'} F_m(\mathbf{H}')F_m(\mathbf{H}-\mathbf{H}') + (2\Theta/V) \sum_{H'} F_m(\mathbf{H}')F_s(\mathbf{H}-\mathbf{H}') + (\Theta/V) \sum_{H'} F_s(\mathbf{H}')F_s(\mathbf{H}-\mathbf{H}') \quad . \qquad (8)$$

Here subscript m stands for main reflections while subscript s stands for satellites. Since the intensities of satellites are on average much weaker than those of main reflections, the last summation on the right-hand side of (8) is negligible in comparison with the second, while the last two summations on the right-hand side of (8) are negligible in comparison with the first. Letting $F(\mathbf{H})$ on the left-hand side of (8) represents only the structure factor of main reflections we have to first approximation

$$F_m(\mathbf{H}) \approx (\Theta/V) \sum_{H'} F_m(\mathbf{H}')F_m(\mathbf{H}-\mathbf{H}') \quad . \qquad (9)$$

On the other hand, if $F(\mathbf{H})$ on the left-hand side of (8) corresponds only to satellites, it follows that

$$F_s(\mathbf{H}) \approx (2\Theta/V) \sum_{H'} F_m(\mathbf{H}')F_s(\mathbf{H}-\mathbf{H}') \quad . \qquad (10)$$

Notice that in this case the first summation on the right-hand side of (8) has vanished, because any three-dimensional reciprocal lattice vector corresponding to a main reflection will have zero components in the extra dimensions so that the sum of two such lattice vectors could never give rise to a lattice vector corresponding to a satellite. An exception to this can be found only when the average structure itself is a four- or higher-dimensional periodic structure as in the so-called composite structures, the analysis of which will be discussed in the lecture given by Prof. Beurskens in this Workshop. Equation (9) indicates that the phases of main reflections can be derived by a conventional direct method neglecting the satellites. Equation (10) can be used for the phase extension from the main reflections to the satellites. This provides a way to determine directly the modulation functions.

Structure details of the incommensurate modulation of the Pb-doped $Bi_2Sr_2Ca_2Cu_3O_X$ high-Tc superconductor have been revealed for the first time using this method (Mo, Cheng, Fan, Li, Sha, Zheng, Li & Zhao, 1992). Since single crystals suitable for X-ray diffraction analysis are extremely difficult to prepare for this compound, electron diffraction instead of X-ray diffraction was used. One dimensional modulation is found from the electron diffraction pattern. All reflections can be indexed using four-integer indices. The *0klm* electron diffraction pattern were measured yielding intensities for 42 main reflections and 70 first order satellites. The phases of main reflections were calculated from the known average structure (Sequeira, Yakhmi, Iyer, Rajagopal & Sastry, 1990), while the phases of satellite reflections were derived by the phase extension according to (10). A Fourier map was then calculated which is the four-dimensional potential distribution function projected along the **a** axis. By cutting this Fourier map perpendicular to the fourth dimension we obtain the projection of the incommensurate modulated structure along the **a** axis in the three-dimensional real space. The result is shown in fig. 3, in which ten unit cells of the average structure are plotted along the **b** axis showing how the atoms are modulated from one unit cell to the other. Both occupational and positional modulations are evident for Bi atoms. The strong occupational modulation of Bi implies large amount of Bi-vacancies disordered on the planes normal to the **b** axis. The same feature is also seen for Ca and Sr atoms. Another prominent feature in fig. 3 is that oxygen atoms of the Cu(1)-O layer move towards the Ca layers forming a disordered oxygen bridge across the layers of Cu(2)-Ca-Cu(1)-Ca-Cu(2). In addition, occupational and positional modulations along the **b** axis are also found for the disordered oxygen atoms. The disordered arrangement and modulation of oxygen atoms imply large amount of O-vacancies on the Cu(1)-O plane.

3.2 Direct methods for combining electron diffraction and electron microscopy

Crystalline materials important in science and technology, such as high-Tc superconductors, are often too small in grain size and too imperfect in periodicity to carry out an X-ray single crystal analysis, but they are suitable for electron microscopic observation. The electron microscope is the only instrument which can produce simultaneously for a crystalline sample a micrograph and a diffraction pattern corresponding to atomic resolution. In principle, either the electron micrograph or the electron diffraction pattern could lead to a structural image.

Dorset (1991) showed that a direct-method electron diffraction analysis, based on the kinematic diffraction approximation, can be a powerful tool for crystal structure analysis. However, the phase problem in electron diffraction analysis is nothing like as easy to solve as it is in X-ray analysis. Electron diffraction patterns provide only a partial set of three-dimensional

reflections within a reciprocal sphere. This weakens the power of direct methods, since the number of phase relationships will be much decreased and some of the strongest relationships might be lost. In addition, the measurement of diffraction intensities is distorted by dynamical diffraction effects and the available techniques of intensity measurement do not compete in accuracy with those available for X-rays. This means that there are considerable difficulties in applying direct-methods to electron diffraction analysis.

High resolution electron microscopy has made great progress in recent years in the study of crystalline materials (Li, 1990). It still has two major disadvantages:

i) in most cases a high resolution electron micrograph does not directly reveal the true structure; what is obtained is a convolution of the structural image with the Fourier transform of a contrast transfer function. Hence some technique is needed to restore the blurred image.

ii) the point-to-point resolution of the micrograph is insufficient to resolve individual atoms in most cases. Hence some procedure is required to enhance the resolution.

The above problems can be solved by combining the information from an electron micrograph with that from the corresponding electron diffraction pattern. Direct methods play an important role in such a combination. Details of the technique will be described in the lecture by Prof. Li in this Workshop. A program is now writing for the electron crystallographic image processing and is hopefully to be released by the end of this year.

3.3 Direct phasing of one-wavelength anomalous scattering (OAS) data from proteins

Multiple isomorphous replacement is now dominating the structure analysis of proteins with no structural precedent. It may occur that the derivatives are difficult to prepare, or they are not isomorphous with the native protein. In this case multi-wavelength anomalous scattering (MAS) can in principle be used, if there are some suitable heavy atoms in the native protein or its non-isomorphous derivative. However MAS technique suffers from the difficulty of collecting and scaling data at different wavelengths accurately. OAS technique does not have this difficulty but it leads to the problem of phase ambiguity. There were several early proposals to use direct methods to break the phase ambiguity inherent in the OAS technique (Fan, 1965; Hazell, 1970; Sikka, 1973; Heinerman, Krabbendam, Kroon & Spek 1978). The method of Fan (1965) has been extended and tested with experimental protein diffraction data. Details of the method are given here. The phase doublet from OAS is expressed as

$$\varphi_H = \varphi''_H \pm |\Delta\varphi_H| \quad , \tag{11}$$

where φ''_H is the phase of

$$\mathbf{F}''_{ano} = \sum_j \; i\Delta f''_j \exp(i2\pi \mathbf{H}.\mathbf{r}_j) = |\mathbf{F}''_{ano}|\exp(i\varphi''_H)$$

$|\Delta\varphi_H|$ is calculated by

$$|\Delta\varphi_H| = |\cos^{-1}\{(F^+ - F^-)/2|\mathbf{F}''_{ano}|\}| \quad .$$

By introducing the concept of best phase, $\varphi_{H,best}$, and figure of merit, m_H , used in protein crystallography into the direct-method approach for dealing with enantiomorphous phase ambiguity (Fan, Han & Qian, 1984), there is obtained

$$\Delta\varphi_{H,best} = \varphi_{H,best} - \varphi''_H \quad , \tag{12}$$

$$\tan(\Delta\varphi_{H,best}) = 2(P_+ - 1/2)\sin|\Delta\varphi_H| \big/ \cos\Delta\varphi_H \tag{13}$$

and

$$m_H = \exp(-\sigma^2_H/2)\,\{[2(P_+ - 1/2)^2 + 1/2](1 - \cos 2\Delta\varphi_H) + \cos 2\Delta\varphi_H\}^{1/2} \quad , \tag{14}$$

where σ^2_H is related to the experimental error and can be calculated from the men square of the "lack of closure error" (Blow & Crick, 1959). The probability that $\Delta\varphi_H$ is positive, P_+ is given by

$$P_+ = (1/2) + (1/2)\tanh\{\sin|\Delta\varphi_H| \times$$

$$[\sum_{H'} m_{H'} m_{H-H'} \kappa_{H,H'} \sin(\Phi'_3 + \Delta\varphi_{H',best} + \Delta\varphi_{H-H',best}) + \chi\sin\delta_H]\} \quad , \tag{15}$$

where

$$\Phi'_3 = -\varphi''_H + \varphi''_{H'} + \varphi''_{H-H'} \quad ,$$

$$\chi = 2|E_H E_{H,ano}| \big/ \sigma_u \quad ,$$

$$\delta_H = \varphi_{H,R} - \varphi''_H \quad .$$

In the above expressions, $E_{H,ano}$ is the contribution of the anomalous scatterers to the normalized

structure factor E_H; $\sigma_u = \Sigma_u (Z_u)^2/\sigma_2$, Z_u is the atomic number of the u^{th} atom which belongs to the unknown part of the structure, and $\sigma_2 = \Sigma_j (Z_j)^2$; $\varphi_{H,R}$ is the phase contributed from the real part scattering of the anomalous scatterers. A procedure for using (12) - (15) is now described. Values of $\Delta\varphi_{H,best}$ and m_H are calculated for each reflection using (13) and (14), assuming that $P_+ = 1/2$. The values of $\Delta\varphi_{H,best}$ and m_H are then substituted into (15) to obtain for each reflection a new P_+, which will mostly differ from 1/2. Substituting the new values of P_+ into (13) and (14) gives an improved set of $\Delta\varphi_{H,best}$ and m_H. Next $\varphi_{H,best}$ is calculated from $\Delta\varphi_{H,best}$ from (12) and values of $\varphi_{H,best}$ and m_H are then used with the observed structure-factor magnitudes to calculate the best Fourier map.

The above procedure has been tested (Fan, Hao, Gu, Qian, Zheng & Ke, 1990) with the experimental OAS data from the Hg-derivative of the protein aPP (Blundell, Pitts, Tickle, Wood, & Wu, 1981). The sample crystallizes in space group C2 with unit cell dimensions a=34.18, b=32.92 c=28.44Å and β=105.30° and with one molecule of 36 amino-acid residues in the asymmetric unit. Diffraction data were collected with CuK_α radiation and 2108 independent reflections at 2Å resolution were observed and used in the test calculation. The resultant direct-method phases led to an interpretable electron density map, a part of which is shown in fig. 4. The correlation coefficient between the electron density map phased by the direct method and that calculated from the true phases is 0.70. The mean phase error of the direct-method phases in comparison with the true phases is 38.4° for the total of 2108 independent reflections at 2Å resolution. Test with another known protein of moderate size is now undertaking.

References

Blow, D.M. & Crick, F.H.C. (1959), *Acta Cryst*. **12**, 794-802.

Blundell, T.L., Pitts, J.E., Tickle, I.L., Wood, S.P. & Wu, C.W. (1981). *Proc. Natl. Acad. Sci*. USA, **78**, 4175-4179.

Cochran, W. (1955). *Acta Cryst*. **8**, 473-478.

Debaerdemaeker, T., Tate, C. & Woolfson, M.M. (1985). *Acta Cryst*. A**41**, 286-290.

Debaerdemaeker, T., Tate, C. & Woolfson, M.M. (1988). *Acta Cryst*. A**44**, 353-357.

Dorset, D.L. (1991). *Ultramicroscopy* **38**, 23-40.

Fan, H.F. (1965). *Acta Phys. Sin*. **21**, 1114-1118. (In Chinese) (An English translation can be found in *Chinese Physics* (1965) 1429-1435)

Fan, H.F., Han, F.S. & Qian, J.Z. (1984). *Acta Cryst*. A**40**, 495-498.

Fan, H.F., Hao, Q., Gu, Y.X., Qian, J.Z. Zheng, C.D. & Ke, H.M. (1990). *Acta Cryst.* A**46**, 935-939.

Germain, G. & Woolfson, M.M. (1968). *Acta Cryst.* B**24**, 91-96.

Hao, Q., Liu, Y.W. & Fan, H.F. (1987). *Acta Cryst*. A**43**, 820-824.

Hazell, A.C. (1970). *Nature Lond*. **227**, 269.

Heinerman, J.J.L., Krabbendam, H., Kroon, J. & Spek, A.L. (1978). *Acta Cryst*. A**34**, 447-450.
Janner, A. & Janssen, T. (1977). *Phys. Rev. B*, **15**, 643-658.
Karle, J. & Hauptman, H. (1956). *Acta Cryst*. **9**, 635-651.
Li, F.H. (1990). *Proc. International Workshop on Electron Crystallography*, Erice, Italy, pp. 153-168.
Mo, Y.D., Cheng, T.Z., Fan, H.F., Li, J.Q., Sha, B.D., Zheng, C.D., Li, F.H. & Zhao, Z.X. (1992). *Supercond. Sci. Technol*. **5**, 69-72.
Sayre, D. (1952). *Acta Cryst*. **5**, 60-65.
Sequeira, A., Yakhmi, J.V., Iyer, R.M., Rajagopal, H. & Sastry, P.V.P.S.S. (1990). *Physica C* **167** 291-296.
Sikka, S.K. (1973). *Acta Cryst*. A**29**, 211-212.
Wolff, P.M.de (1974). *Acta Cryst*. A**30**, 777-785.
Wolff, P.M.de, Janssen, T. & Janner, A. (1981). *Acta Cryst*. A**37**, 625-636.
Yao, J.X. (1981). *Acta Cryst*. A**37**, 642-644.

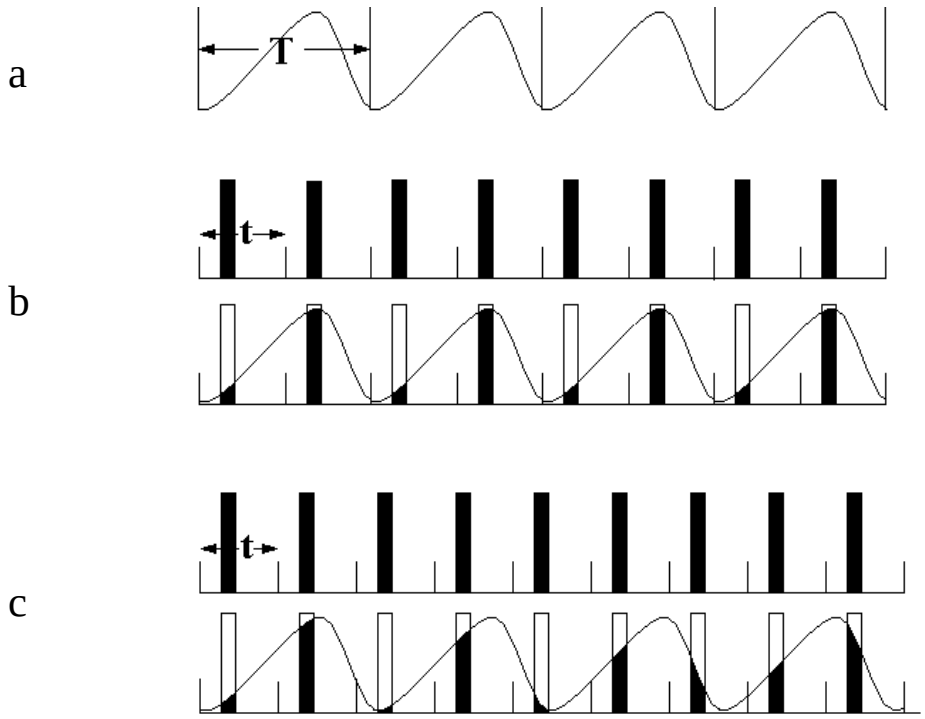

Figure 1. Occupational modulation of a one-dimensional structure
(a) modulation wave with a period equal to **T**; (*b*) upper row: one-dimensional regular structure with atoms shown as thick vertical lines and with a period equal to **t**; lower row: the resulting commensurate modulated structure; (*c*) upper row: one-dimensional regular structure; lower row: the resulting incommensurate modulated structure

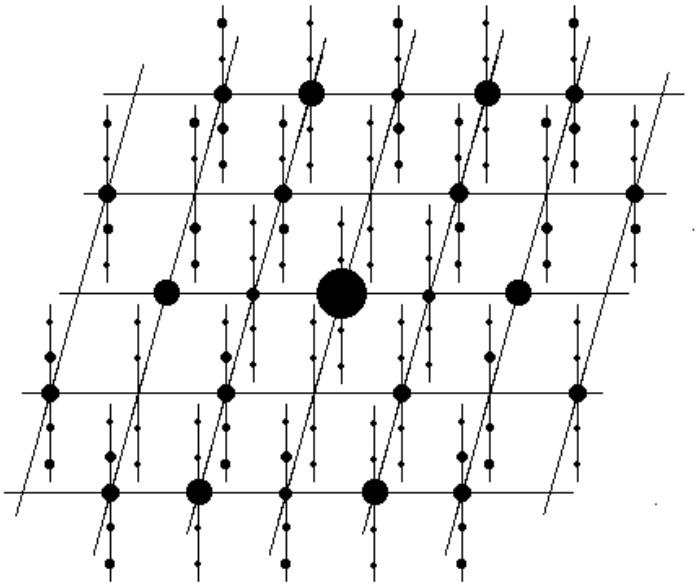

Figure 2. Schematic diffraction pattern of an incommensurate modulated structure
The vertical line segments indicate projected lattice lines parallel to the fourth dimension

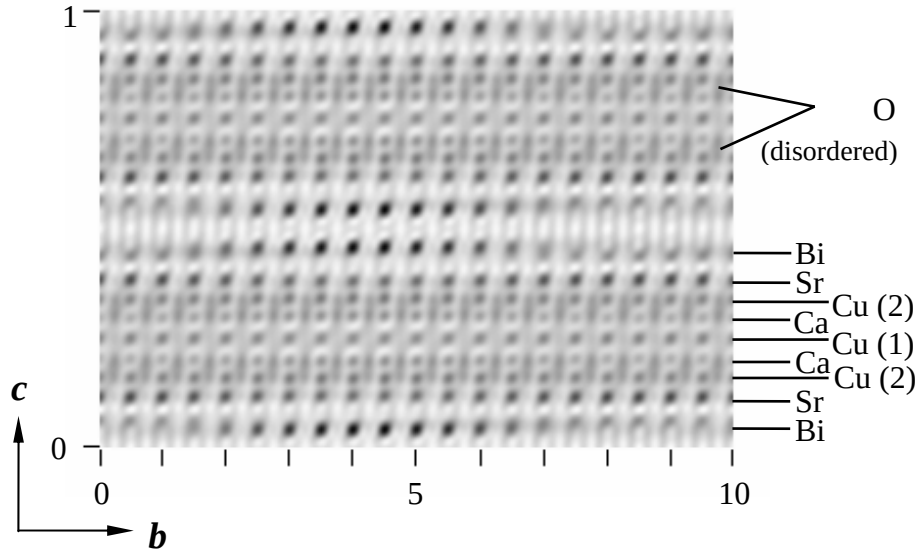

Figure 3. The 3-dimensional potential distribution function of the Pb-doped Bi-2223 superconductor projected along the **a** axis. Ten unit cells are plotted along the **b** axis, showing the period of modulation to be approximately 8.5 times the length of **b**.

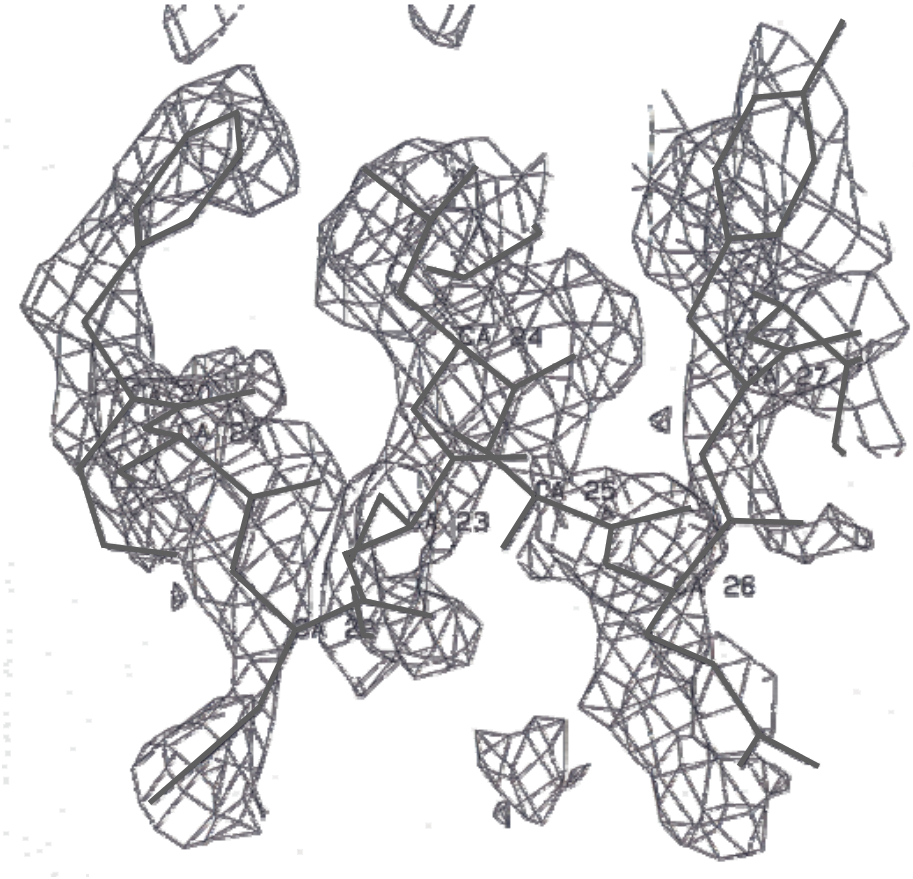

Figure 4. Portion of the electron-density map for aPP calculated with phases derived by using equations (12) - (15)